A Simulation Model of Aerosol Collection in Granular Media

HEMANT PENDSE[1] AND CHI TIEN

Department of Chemical Engineering and Materials Science, Syracuse University, Syracuse, New York 13210

Received March 13, 1981; accepted September 17, 1981

A simulation model for aerosol collection in granular media resulting from the flow of aerosol streams is proposed. The granular medium is represented by the recently proposed constricted tube model which takes into account the divergent–convergent flow characteristics of porous media and the interaction of neighboring grains. The deposition process is described by the following assumptions: (a) the aerosol particles are randomly distributed in the streams and (b) once a particle becomes collected, it may act as a collector itself, thereby leading to the formation and growth of particle aggregates as deposits. For a given set of operating conditions, the model provides detailed information about the dynamics of the deposition process including the number of particles collected, and the position of the deposited particle as functions of time. Application of the model to granular filtration design is discussed. Generally speaking, the results of the stimulation model can be used to develop a relationship between changes in collection efficiency and pressure drop and the extent of particle collection, thus making it possible to predict the dynamic behavior of the filtration process. Comparison between the model and experimental results is also presented.

INTRODUCTION

The application of deep granular beds for the removal of small particles from gaseous streams is an old and yet often-overlooked engineering practice. A survey conducted (1) in 1973 indicated that granular filtration is used extensively in a large number of major industries with its first application dating back almost a century ago. In more recent years, much discussion has been given to the possible use of granular filtration in high-temperature and high-pressure gas cleaning. It is generally recognized that high-temperature gas cleaning technology is essential to the successful development of combined-cycle power generation systems.

Paradoxically, relatively little attention has been given to studies concerning the nature and mechanism of granular filtration. Most of the earlier literature in this area was concerned with operating problems. A few recent investigations (2–5) have considered the dynamics of particle deposition in granular media during the initial stage of filtration process (i.e., when the media is relatively free of deposited particles). The paradigm necessary for the rational design of granular filtration is yet to be formulated.

When a gas–solid suspension flows through a filter bed, particle deposition takes place throughout the bed under the influence of a variety of forces acting on the particles present in the suspension. As deposited particles accumulate within the bed, the media structure undergoes a continuous change. Both the collection efficiency of the bed and the pressure drop across the bed necessary to maintain a constant flow rate of the suspension vary with time. The study of the dynamic behavior of granular filtration is, in essence, the prediction of the transient behavior as the bed becomes increasingly clogged.

The purpose of the present study is the formulation of a simulation model describing the complete dynamics of aerosol filtration in granular beds. The model is potentially capable of predicting the rate of particle deposition as a function of time

[1] Present address: Department of Chemical Engineering, University of Maine, Orono, Maine 04473.

0021-9797/82/050225-17$02.00/0

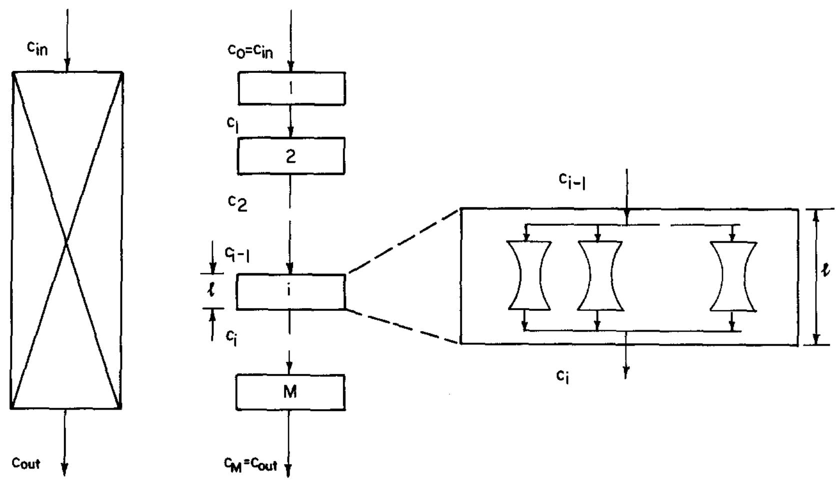

FIG. 1. Schematic representation of a granular filter bed.

(or alternatively the increase in the collection efficiency as a function of the extent of deposition) and the morphology of particle deposits as well as its evolution. Together with a recently proposed semiempirical procedure which calculates the increase in drag force due to deposited particles on collectors (6) the pressure drop increase across the bed as the bed becomes clogged can also be estimated. To the authors' knowledge, this work represents the first attempt at studying the transient behavior of granular filtration in a fundamental manner.

The formulation of the simulation model is based on the general principles proposed earlier (7, 8) for particle deposition on single collectors. The paper is divided into three parts. First the formulation of the model with the use of the constricted tube model for the characterization of granular bed is described. Second, the treatment of the simulation results and their potential applications are presented. Finally, the possible modifications of the model are discussed. Comparison between the model and experimental data suggests that the model is indeed a viable tool for the study of the transient behavior of granular filtration.

GEOMETRICAL REPRESENTATION OF GRANULAR BEDS

The simulation model is formulated on the basis that a granular filter bed can be represented by the constricted tube model proposed by Payatakes *et al.* (9). Accordingly, a filter bed can be viewed as a number of unit bed elements (UBE) of thickness, l, connected in series. Within each unit bed element, there exists a number of unit collectors (denoted by N_c, the number of constricted tubes per unit cross-sectional areas) in the shape of constricted tubes. For simplification all the unit collectors are assumed to be identical in size and shape. The dimensions of the constricted tube are described by its height, h, the maximum diameter, d_m, and the constriction diameter, d_c. The schematic representation of filter beds by the constricted tube model parameters and the macroscopic properties of porous media as formulated by Payatakes *et al.* are summarized in Table I. (Also see Fig. 1.)

To complete the description, the shape of the wall of the constricted tube needs to be specified. In the original formulation of Payatakes *et al.* (9) the tube wall is assumed to be parabolic. Subsequent investigators have suggested the use of other

TABLE I

Determination of Constricted Tube Model Parameters (Case of Uniform Unit Cell Size)

(1) Number of constricted tubes per unit area, N_c

$$N_c^* = N_c \cdot d_g^2 = \frac{6 \cdot \epsilon^{1/3} (1 - S_w)^{1/3} \cdot (1 - \epsilon)^{2/3}}{\pi}$$

(2) Length of unit bed element,

$$l^* = \frac{l}{d_g} = \left[\frac{\pi}{6} \frac{1}{(1 - \epsilon)}\right]^{1/3}$$

(3) Constriction diameter, d_c[a]

$$d_c^* = \frac{d_c}{d_g} = 2r_1^* = 0.35 \text{ (approximately)}$$

(4) Height of the unit cell, h

$$h = d_g$$

(5) Maximum diameter of the unit cell, d_m

$$d_m^* = \frac{d_m}{d_g} = 2r_2^* = \left[\frac{(1 - S_{wi})}{(1 -)}\right]^{1/3}$$

[a] d_c and S_{wi} can be determined from capillary pressure-saturation data (9).

geometries (10, 11). For the present work, the tube geometry is considered to be either parabolic or sinusoidal. In other words, the dimensionless diameter of the constricted tube wall, d/d_g is given as

Parabolic Geometry

$$d^* = \frac{d}{d_g} = \frac{1}{d_g}\left[d_c + 4(d_m - d_c)\left(\frac{z}{h} - \frac{1}{z}\right)^2\right] \quad [1]$$

Sinusoidal Geometry

$$d^* = \frac{d}{d_g} = \frac{1}{d_g}\left[\frac{d_c + d_m}{2} + \frac{d_m - d_c}{2} \times \cos\left(2\pi \frac{z}{h}\right)\right]. \quad [2]$$

The flow field expression inside the parabolic constricted tube was first obtained by Payatakes *et al.* (12) numerically. Subsequently, Neira and Payatakes (13) presented approximate solution using the collocation method. The solution of Neira and Payatakes was used in the present study because of its accuracy and simplicity. For the sinusoidal constricted tube, the flow field expression was obtained from the perturbation solution given by Chow and Soda (14). Unlike the collocation solution, the perturbation solution is valid up to moderate Reynolds number and incorporates the effect of fluid inertia. The use of different geometries gives rise to different flow fields within the unit collector. A recent study (2) has shown that this difference may be an important factor in the application of this geometric model for the study of particle deposition in granular filters.

FORMULATION OF THE SIMULATION MODEL

With the use of the constricted tube model, aerosol filtration in granular media can be considered as the deposition of particles on the surface of the constricted tube from suspensions flowing through the tube. According to the proposed simulation model, one considers each and every particle entering the tube and determines whether or not a particle will be collected by following its trajectory. In the event that a particle is collected, its position of deposition is recorded and becomes part of the inventory. The procedure for the simulation can be divided into three steps described briefly as follows.

A. Assignment of Initial Positions of Particles at Tube Inlet

The basic assumption used in assigning initial positions for entering particles is that particles enter the tube one at a time and they are randomly distributed at the inlet. For convenience, the initial position can be given in terms of the cylindrical polar coordinates (r_{in}, ϕ_{in}). Let r_0 be the radial distance, beyond which no particle can be placed at the tube entrance. One can obtain r_0 from geometric calculations. In particular, for sinusoidal tubes,

$$2r_0 = d_m - 2a_p \quad [3]$$

where a_p is the particle radius.

For any position (r, ϕ), $0 < r < r_0$, and $0 < \phi < 2\pi$, the probabilility of a particle (in terms of its center) being within an area element $rd\phi dr$ at the inlet is proportional to the volumetric flow rate of the suspension through the area element. Thus one has

$$\text{Probability } (0 < r_{in} < r_0) = 1 \quad [4]$$

$$\text{Probability } (0 < \phi < 2\pi) = 1 \quad [5]$$

$$G_1(r) = \text{Probability } (r_{in} < r) = \frac{\psi(0, r) - \psi(0, 0)}{\psi(0, r_0) - \psi(0, 0)} \quad [6]$$

$$G_2(\phi) = \text{probability } (\phi_{in} \leq \phi) = \frac{\phi}{2\pi} \quad [7]$$

where $\psi(z, r)$ is the stream function corresponding to the flow within the constricted tube of specified tube wall geometry.

From the cumulative density functions $G_1(r)$ and $G_2(\phi)$ of random variables r_{in} and ϕ_{in}, respectively, one can find the random variates in terms of the two uncorrelated random numbers R_1 and R_2 distributed uniformly over (0, 1) as follows:

$$r_{in} = G_1^{-1}(R_1) \quad [8]$$

$$\phi_{in} = G_2^{-1}(R_2) = 2\pi R_2. \quad [9]$$

A standard random number generator (GGUBF) from the International Mathematical and Statistical Library (IMSL) was used to general sets of R_1 and R_2 from which the initial positions of the succeeding entering particles were determined.

B. Determination of Particle Trajectory

Once the initial position of an entering particle is given, its trajectory is known deterministically assuming that the Brownian diffusion effect is negligible. The particle trajectory can be obtained from the integration of the equations of particle motion with the knowledge of the flow field of the fluid.

There are two drawbacks to such an approach. First, the flow field expressions used in this work—the collocation solutions for the parabolic constricted tube and the perturbation solution for the sinusoidal tube—do not take into account of the effect of deposited particles. Furthermore, even if the correct flow field expression were available, it would be time consuming and even prohibitive if the number of entering particles considered is larger. For practical purposes, the particle trajectories should be estimated by certain simple methods rather than performing the integrations involved.

For the present work particle trajectories corresponding to the two limiting cases—extremely high and low particle inertia—will be used. For an entering particle with extremely large inertia, its trajectory will be rectilinear. On the other hand, if it possesses little inertia its trajectory will coincide with the appropriate fluid streamline which can be readily determined by the corresponding flow field expression.

C. Determination of the Outcome of Entering Particles

There are three possible outcomes for any particle entering the unit collector, namely

(i) deposition on the tube wall (primary collection);

(ii) deposition on an already deposited particle (secondary collection);

(iii) escape out of the unit collector.

An entering particle escapes out of the unit collector if the following conditions are satisfied for all points (z, r, ϕ) on its trajectory

$$y(z, r, \phi) > 2d_p \quad [10]$$

and

$$d_i > d_p \quad \text{for all } i \quad [11]$$

where y denotes the normal distance between the point (z, r, ϕ) and the tube wall. d_i is the distance between (z, r, ϕ) and the center of the ith deposited particle recorded in the inventory. The above conditions assume that contact between an entering particle and the wall of the unit collector (or one of the already deposited particles) leads to deposition automatically. The possibility of particles bouncing off upon impact was not considered. This point will be discussed in later sections.

The computation scheme developed to determine the outcome of an entering particle involves essentially the observation of its trajectory as the particle moves through the unit collector to see if either of the two relations, i.e., Eqs. [10] and [11] is not satisfied, indicating particle collection (primary collection by Eq. [10] and secondary collection by Eq. [11]). This is accomplished by incrementing the axial coordinate z, in steps Δz along the particle trajectory. It should be noted that the ϕ coordinate of the particle's center is invariant and remains the same as its inlet value, ϕ_{in}. For high particle inertia, $r = r_{in}$ since the trajectory is rectilinear. On the other hand, if the particle trajectory coincides with fluid streamline, the value of the stream function ψ, along a given trajectory remains the same. Accordingly the coordinates (r, z) of streamline trajectory are related to each other as follows:

$$\psi(z, r) = \psi_{in} \qquad [12]$$

and

$$\psi_{in} = \psi(0, r_{in}). \qquad [13]$$

Thus, with r_{in} known, the value of r for any given value of z can be found readily. As stated before, the stream function is given by the perturbation solution of Chow and Soda (14) for the sinusoidal geometry and the collocation solution of Neira and Payatakes (13) for the parabolic geometry.

TREATMENT OF SIMULATION RESULTS AND THEIR APPLICATIONS

The simulation model yields results in the form of the number of particles collected within a unit collector and their respective positions of deposition as functions of the number of entering particles assuming the dimension and the shape of the unit collector are known. The dynamic behavior of granular bed filtration is characterized by the histories of effluent quality and the pressure drop across the bed necessary to maintain a given flow rate. For the simulation results to be useful in the prediction of the dynamic behavior of granular filtration, the following procedures are developed.

A. *Filter Coefficient, Collection Efficiency, and Their Changes*

The macroscopic behavior of a deep bed filter can be described (15) by the following set of equations

$$V_s \frac{\partial c}{\partial z} + \frac{\partial \sigma}{\partial \theta} = 0 \qquad [14]$$

$$\frac{\partial c}{\partial z} = -\lambda c \qquad [15]$$

where c and σ denote the particle concentration in the suspension and amount of particle deposit per unit bed volume. V_s is the superficial velocity and z and θ are the axial distance and the corrected time respectively (i.e., $\theta = t - \int_0^z \epsilon/V_s dz$). The filter coefficient, λ is related to the collection efficiency of the unit collector, η by the following expression (15)

$$\lambda = \frac{1}{l} \ln \frac{1}{1 - \eta} \qquad [16a]$$

$$\lambda \simeq \frac{\eta}{l} \quad \text{if} \quad \eta \ll 1. \qquad [16b]$$

The simulation model gives the number of particles collected, m_c, as a function of the number of particles entering the unit collector, m_{in}. By definition, the collection efficiency of the unit collector, η is given as

$$\eta = \frac{dm_c}{dm_{in}}. \qquad [17]$$

Accordingly, if the simulation data of m_c vs m_{in} can be fitted by a polynomial expression with appropriate numerical technique as

$$m_c = \sum_{i=1}^{n} a_i m_{in}^i. \qquad [18]$$

The collection efficiency of the unit collector, η becomes

$$\eta = \sum_{i=1}^{n} i a_i m_{\text{in}}^{i-1}. \quad [19]$$

The simulation data therefore can be used readily to determine the filter coefficient with the use of Eqs. [19] and [16a].

The study of the transient behavior of granular filtration requires the knowledge of the dependence of λ (or η) on the extent of deposition. The latter can be described by the specific deposit, σ. The use of Eq. (19) yields values of η throughout the filtration cycle. The corresponding values of σ can be found from the definition of σ, the dimension of the unit collector, and the number of particles collected m_c as

$$\sigma = \frac{\text{volume of particles collected per unit collector}}{\text{volume of filter bed per unit collector}} = \frac{(m_c)\dfrac{4\pi}{3}a_p^3}{(l/N_c)}. \quad [20]$$

The total number of particles entered into the unit, m_{in} up to time θ is given as

$$m_{\text{in}} = \int_0^{\theta} \frac{qc(\theta')\cdot d\theta'}{\dfrac{4\pi}{3}a_p^3} \quad [21]$$

where q is the volumetric flow rate of suspension into the unit collector. q is related to the superficial flow rate through the filter bed, V_s by the expression

$$q = \frac{V_s}{N_c}. \quad [22]$$

The rate of the increase of the specific deposit, $\partial\sigma/\partial\theta$ can be obtained by differentiating Eq. [20] with respect to θ. Utilizing the relationship of Eqs. [17], [21], and [22] the differentiated form of Eq. [20] is found to be

$$\frac{\partial\sigma}{\partial\theta} = V_s\left(\frac{1}{l}\right)\left(\frac{dm_c}{dm_{\text{in}}}\right)c = (V_s)\left(\frac{\eta}{l}\right)\cdot c. \quad [23]$$

From Eqs. [14] and [15], one has

$$\frac{\partial\sigma}{\partial\theta} = V_s\lambda c. \quad [24]$$

A comparison of the above two equations gives

$$\lambda = \frac{\eta}{l}$$

which is the same as Eq. [16b]

B. Pressure Drop History

The increase in pressure drop experienced by a clogged filter bed can be viewed as due to the drag force acting on deposited particles. In a recent study (6), semiempirical methods were developed for the estimation of drag forces acting on spherical particles attached to a larger spherical body. Assuming one can establish an equivalency between the spherical geometry and the constricted tube geometry used in this study, these methods—together with the results of the number of particles collected and their positions of deposition—can be used to estimate the increase in total drag force, which in turn, give the estimate of the pressure drop increase.

First the hydrodynamic drag force acting on a clean unit collector due to suspension flow can be written as

$$F_{D,0} = 3\pi d_g \mu V_s \gamma_0. \quad [25]$$

The quantity $3\pi d_g \mu V_s$ represents the drag force acting on a sphere of diameter d_g

(filter grain diameter) according to Stokes' law. The quantity γ_0 is the ratio of the drag force acting on a clean unit collector and the drag force on a filter grain according to Eq. [25]. γ_0 is found to be (16):

$$\gamma_0 = \frac{F_{\mathrm{D},0}}{3\pi\mu d_{\mathrm{g}} V_{\mathrm{s}}} = \frac{2l^*}{3\pi N_{\mathrm{c}}^*} (f_{\mathrm{s}} \cdot N_{\mathrm{Re_s}}) \quad [26]$$

where l^* and N_{c}^* are the dimensionless values of l and N_{c} (see Table I), f_{s} is the friction factor of the filter bed, and $N_{\mathrm{Re_s}}$ is the Reynolds number based on the filter grain diameter and the superficial velocity of suspension. The value of $f_{\mathrm{s}} \cdot N_{\mathrm{Re_s}}$ can be evaluated from the flow field expressions (i.e., the models used for filter media characterization). A summary of these expressions is given in Table II. For a filter bed composed of glass beads ($d_{\mathrm{g}} \cong 532\ \mu\mathrm{m}$) with $\epsilon_0 = 0.38$, γ_0 is found to be 132 and 125 for the parabolic and sinusoidal constricted tube, respectively.

The drag force increase due to the presence of the ith deposited particle within the unit collector can be expressed as

$$\Delta F_{\mathrm{D},i} = 3\pi\mu d_{\mathrm{p}} V_{\mathrm{s}} \cdot \gamma_i \quad [27]$$

where γ_i is the correction factor relating $\Delta F_{\mathrm{D},i}$ to the Stokes drag force on an isolated sphere, i.e., a single filter grain (or an isolated particle) in an unbounded flow.

The total increase in the drag force due to the presence of all the deposited particles as predicted by the simulation becomes

$$\frac{\Delta F_{\mathrm{D}}}{F_{\mathrm{D},0}} = \frac{N_{\mathrm{R}}}{\gamma_0} \sum_{i=1}^{m_{\mathrm{c}}} \gamma_i. \quad [28]$$

The correction factor, γ_i for the contribution to drag force increase due to the ith deposited particle, $\Delta F_{\mathrm{D},i}$ depends on its position within the tube, the undisturbed fluid velocity evaluated at its center, $V_{(i)}$, and the presence of other deposited particles. Following the established procedures given in Ref. (6) one may write

TABLE II

Expressions of $f_{\mathrm{s}} N_{\mathrm{Re_s}}$ for Different Tube Geometries

Tube geometry	$f_{\mathrm{s}} N_{\mathrm{Re_s}}$
Parabolic	$\dfrac{2(-\Delta p)\langle d_{\mathrm{c}}\rangle \langle d_{\mathrm{g}}^2\rangle}{\pi\, l^* N_{\mathrm{c}}^* \langle d_{\mathrm{c}}^3\rangle}$
Hyperbolic	$\dfrac{24\, g(\xi_0 \zeta_0)}{N_{\mathrm{c}}^*\, d_{\mathrm{c}}^{*4}}$
	$\xi_0 = \left[\left(\dfrac{d_{\mathrm{m}}}{d_{\mathrm{c}}}\right)^2 - 1\right]^{1/2}$
	$\zeta_0 = [(\xi_0 d_{\mathrm{c}}^*)^2 + 1]^{-1/2}$
	$g(\xi_0, \zeta_0) = \dfrac{1}{\xi_0\zeta_0} - \dfrac{(1+\zeta_0)^2}{(1+2\zeta_0)} \times \left[\dfrac{\xi_0}{1+\xi^2} + \tan^{-1}\xi_0\right]$
Sinusoidal	$(f_{\mathrm{B}} N_{\mathrm{ReB}})^a \dfrac{(1-\epsilon)^2}{2\epsilon^3}$

[a] The quantity $(f_{\mathrm{b}} \cdot N_{\mathrm{ReB}})$ as a function of parameters characterizing the dimensions of the unit cell; involving d_{c}^* and d_{m}^* is given by Fedkiw and Newman (10).

$$\gamma_i = \frac{\Delta F_{\mathrm{D},i}}{3\pi\mu d_{\mathrm{p}} V_{\mathrm{s}}} = \frac{[3\pi\mu d_{\mathrm{p}} V_{(i)}] \cdot f(\bar{r}_i, \bar{r}_j) \cdot f(\bar{r}_i, \bar{r}_k)}{3\pi\mu d_{\mathrm{p}} V_{\mathrm{s}}} = \left(\frac{V_{(i)}}{V_{\mathrm{s}}}\right) \cdot f(\bar{r}_i, \bar{r}_j) \cdot f(\bar{r}_i, \bar{r}_k) \quad [29]$$

where the jth and kth deposited particles are the two closest neighbors of the ith particle. $\bar{r}_i$, $\bar{r}_j$, and $\bar{r}_k$ are the position vectors of the ith, jth, and kth deposited particle, respectively. The function f takes into account the two-particle interaction effect and is given in Ref. (6).

The relative increase in pressure drop of a clogged filter bed can be related to the relative increase in drag force due to the presence of the deposited particles within a unit collector, or

$$\frac{\partial p/\partial z}{(\partial p/\partial z)_0} - 1 = \frac{F_{\mathrm{D},0} + \sum_{i=1}^{m_{\mathrm{c}}} (\Delta F_{\mathrm{D},i})}{F_{\mathrm{D},0}} - 1. \quad [30]$$

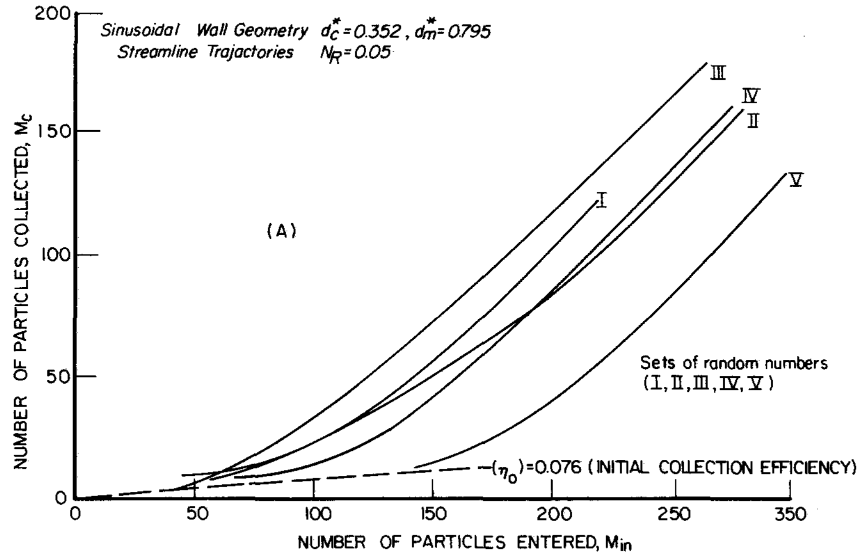

FIG. 2. Stochastic variability of simulation results, M_c vs M_{in}.

Substituting Eqs. (25)–(29) into Eq. (30), the final expression is found to be

$$\frac{\left(\frac{\partial p}{\partial z}\right)}{\left(\frac{\partial p}{\partial z}\right)_0} - 1 = N_R\left(\frac{3\pi N_c^* f_s N_{Re_s}}{2l^*}\right) \times \sum_{i=1}^{m_c} \frac{V_{(i)}}{V_s} f(\bar{r}_i, \bar{r}_j)\cdot f(\bar{r}_i, \bar{r}_k). \quad [31]$$

SIMULATION RESULTS

A brief discussion of the simulation results is given below. A more detailed description can be found in Pendse's dissertation (16).

A. Internal Consistency of the Simulation Model

The simulation model presented above has the potential capability of yielding all the pertinent information concerning particle deposition in granular media. A check of its internal validity is, however, a prerequisite for its application to the study of deep bed filtration. Such a check can be performed by studying (a) the stochastic

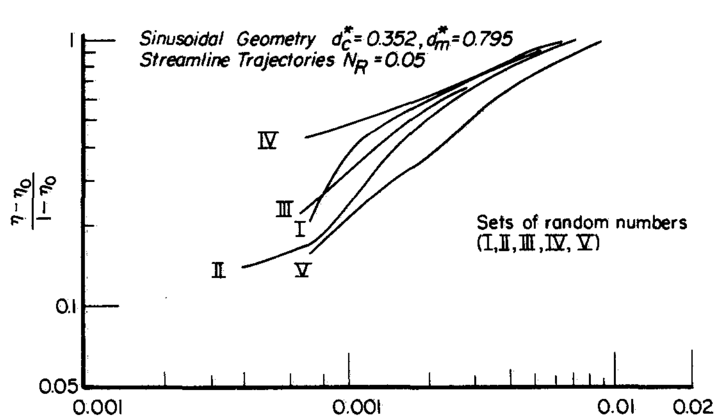

FIG. 3. Stochastic variability of simulation results, η vs σ data.

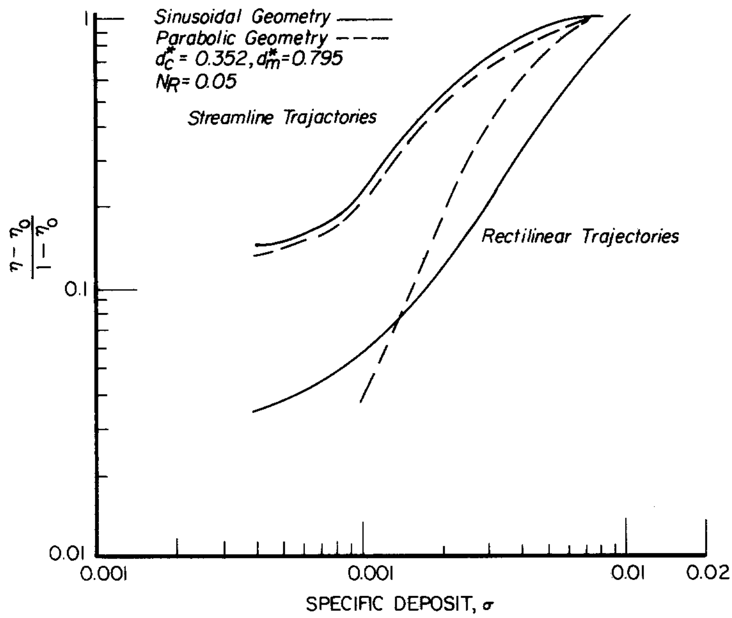

FIG. 4. Effect of tube geometry on simulation results.

variability, and (b) the sensitivity to the tube geometry. These two problems will be considered separately.

Stochastic variability. A number of replicate runs were made using different sets of random numbers to determine the initial positions of approaching particles. Figure 2 shows m_c vs m_{in} data for five replicate runs. These runs were made with the use of the sinusoidal geometry, with $N_R = 0.05$ and the assumption that particles move along fluid streamlines. The corresponding results of η vs σ are shown in Fig. 3. It is clear that in spite of the stochastic variations, the m_c vs m_{in} and η vs σ relationships follow a common trend. Quantitative comparisons with experimental data, thus, can be made by using the ensemble average of the simulation results of replicate runs.

Sensitivity to the tube geometry. Two types of constricted tube geometries, namely, the sinusoidal and parabolic, were used to study the effect of tube geometry on the simulation results. Figure 4 shows the increase in the collection efficiency due to deposition expressed as $(\eta - \eta_0)/(1 - \eta_0)$ vs σ, where η_0 is the clean collector efficiency for these two geometries corresponding to the two limiting cases of particle trajectory at fixed $N_R (N_R = 0.05)$. The effect of the wall geometry appears to be less significant than that of the type of particle trajectory. In the case of streamline trajectories, the effect of the wall geometry is essentially negligible. To determine the possible effect of the dimensions of the constricted tube on the change of η vs σ, the results corresponding to two kinds of granular beds are shown in Fig. 5. The effect of the tube dimensions appears to be negligible.

B. Effect of Particle Size and Particle Size Distribution

Particle size. The particle size, or more appropriately, the ratio of the size of the particle to that of the filter grain, N_R, is an important factor concerning the deposition process. It is the dimensionless parameter which determines the contribution to particle collection by the interception effect. Beizaie (17) has shown that the extent of the shadow effect is determined by the value of N_R. The simulation model developed in

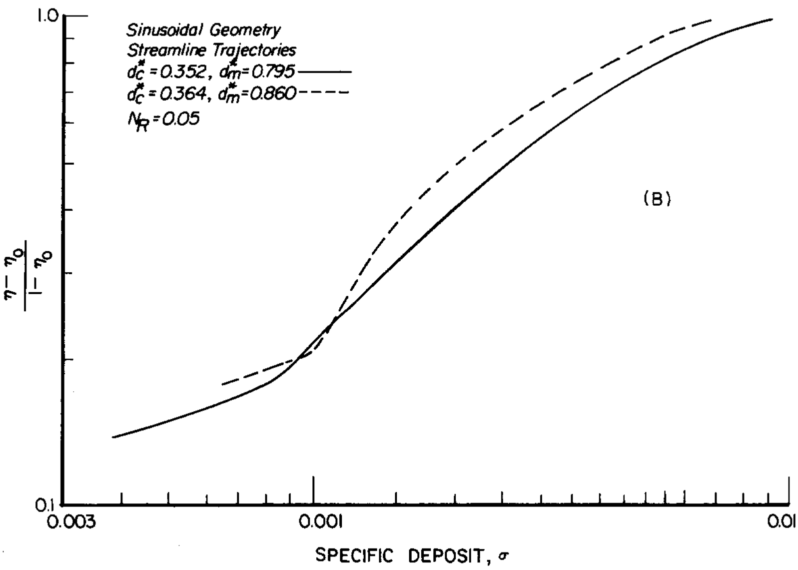

FIG. 5. Effect of unit cell dimensions on simulation.

this work affords an opportunity to study the effect of N_R on the deposition process in its entirety, including both the change of the collection efficiency and the increase in pressure drop.

The effect of N_R on the dependence of η on σ is shown in Fig. 6. The simulation results presented in this figure were obtained using the sinusoidal geometry with $d_c^* = 0.352$ and $d_m^* = 0.795$, and with both streamline and rectilinear particle trajectories. The variation of η vs σ, is represented in the form of $(\eta - \eta_0)/(1 - \eta_0)$ vs σ. The results suggest that for large particles (or large N_R) the effect of N_R is more pronounced at low degree of deposition. At high degree of deposition the effect of N_R becomes less important. This is true for both types of particle trajectories.

Particle size distribution. In practical applications, particles in suspension are likely to be nonuniform in size. Although it is often possible to approximate particles of different sizes by their average size, suspensions containing particles with the same mean particle size would not necessarily behave the same way. The spread of particle size is obviously an important factor.

The simulation model developed in this work can be readily applied to study the effect of particle size distribution on particle deposition. The procedure described earlier can be easily modified to account for the fact that the particles are not uniform in size. The probability of an approaching particle to be of a given size is therefore related to the size distribution density function. Let $G_3(d)$ be the cumulative distribution function for particle diameter, d_p, or

$$\text{probability } (d_p \leq d) = G_3(d). \qquad [32]$$

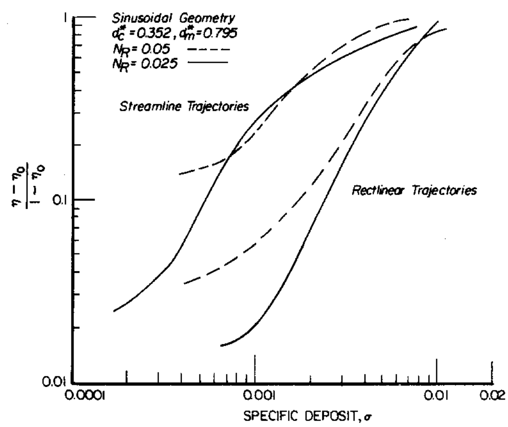

FIG. 6. Effect of particle size on simulation.

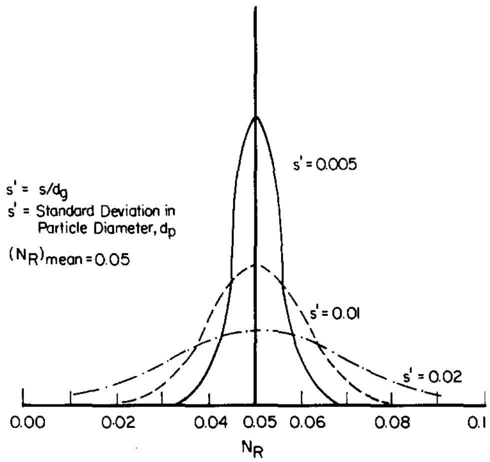

FIG. 7. Normal probability distribution function for particle size distribution.

Then one can generate d_p from a basic random number R_3, uniformly distributed over (0, 1) as follows:

$$d_p = G_3^{-1}(R_3). \quad [33]$$

If one assumes that the particle size distribution is approximately normal, G_3 becomes

$$G_3(d) = \int_{\infty}^{d} \frac{1}{s 2^{1/2}} \times \exp\left\{ -\frac{1}{2} \frac{(x - d_{p,\text{mean}})^2}{s^2} \right\} dx \quad [34]$$

where $d_{p,\text{mean}}$ is the mean particle diameter, and s is the standard deviation. Equations [33] and [34] together relate d_p to basic uniform random numbers. More conveniently, one can generate d_p using the standardized normal random number, Z (which can be generated using IMSL subroutine GGNOF), together with the following relationship

$$d_p = d_{p,\text{mean}} + s \cdot Z. \quad [35]$$

The assignment of the initial positions of approaching particles at the tube entrance and the determination of the outcome follow essentially the same procedure as described before with the following obvious modification: the condition for particle deposition on ith deposited particle is that the center to center between the two particles be equal to $(d_p + d_{p,i})/2$ (see Eq. [11]). The assign-

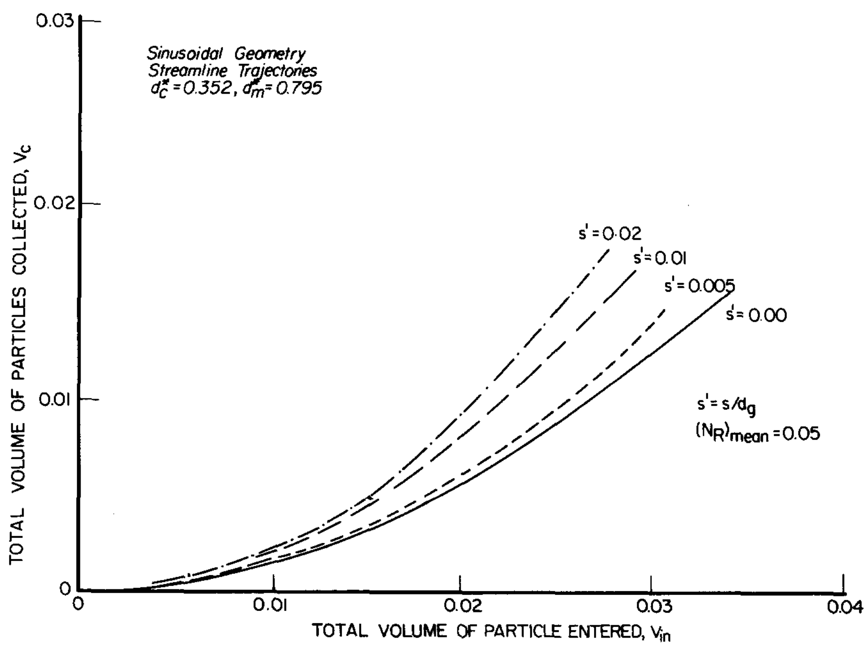

FIG. 8. Effect of particle size distribution on deposition.

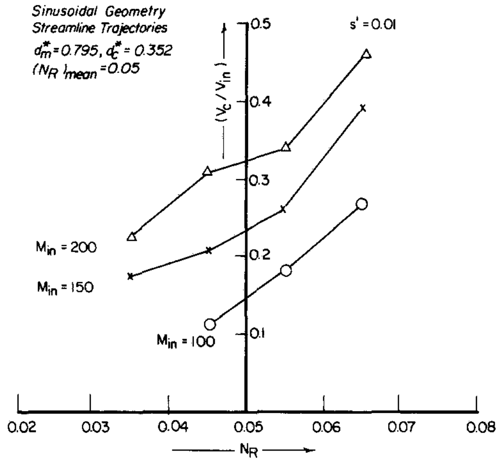

FIG. 9. Collection efficiency of various size fractions of polydisperse suspension.

ment of particle size follows the procedure just described.

A case study of the effect of particle size distribution on the deposition process is presented below. Three specific size distributions are considered (see Fig. 7). The mean particle diameter is $0.05d_g$ and the standard deviations are $0.005d_g$, $0.01d_g$, and $0.02d_g$, respectively. The sinusoidal geometry and streamline particle trajectories are used. The results are presented in Fig. 8, in which the total amount of particles collected (expressed in terms of total volume of deposited particles) is shown as a function of total particles entered (expressed in terms of total volume of particle entered into the cell). Analogous to the definition of η given by Eq. [17], the instantaneous collection efficiency η can be written as

$$\eta = \frac{dV_c}{dV_{in}} . \qquad [36]$$

The initial collection efficiency, η_0, does not appear to be strongly influenced by the spreadness of particle size distribution (i.e., the value of standard deviation). On the other hand, the change of the collection efficiency with substantial deposition is more pronounced if the size range of particles becomes greater. It is obvious that there is a preferred collection of large particles as shown in Fig. 9 which shows the ratio of the total volume of collected particles to that of the entering particles corresponding to various size fractions of a polydisperse suspension as a function of N_R.

C. Distribution of the Deposited Particles within the Constricted Tube

One of the potentially important features of the simulation model is its capacity of providing detailed data about the morphology of the deposit from the information of the position of the deposited particles. In an earlier study, Beizaie (17) proposed the three-stage hypothesis for the deposition process, namely

(1) attachment of particles at discrete points on filter grains—clean filter stage

(2) particle deposition onto already deposited particles to form dendrites—dendrite growth stage

(3) open structured solid growth, when individual dendrites are undistinguishable from each other—open structured solid growth stage.

The simulation results obtained in this work confirm this hypothesis. A typical set

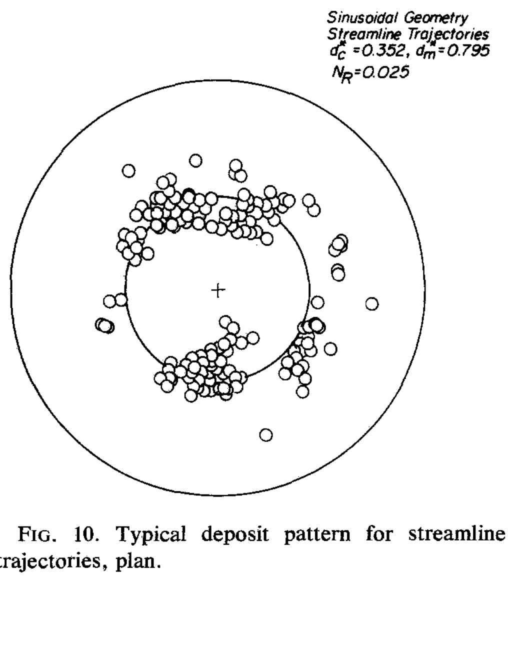

FIG. 10. Typical deposit pattern for streamline trajectories, plan.

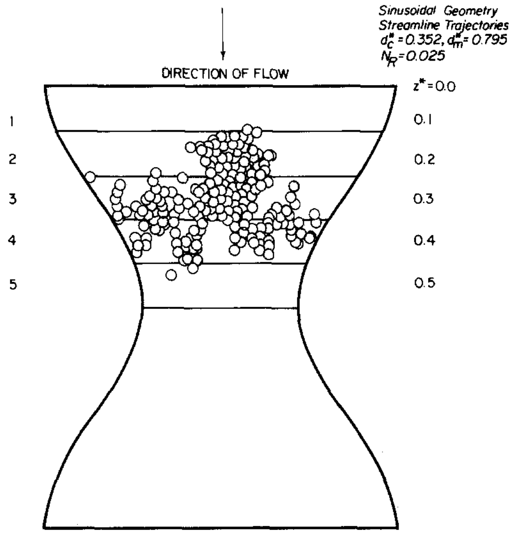

FIG. 11. Typical deposit pattern for streamline trajectories, elevation.

of results is presented in Figs. 10, 11, and 12 in which various views of the deposits in a unit cell for the case of $N_R = 0.025$, based on streamline particle trajectories and sinusoidal geometry, are shown. Figures 10, 11, and 12 give the plan, elevation, and side view for a deposit pattern corresponding to specific deposit of 0.0016. Further examination of the data clearly indicates that the deposit is far from being uniform. There is no deposition in the downstream half of the tube and the deposit growth is directed toward the tube entrance and the tube axis, resulting in continuous narrowing of the available area for flow. A comparison of results obtained using different particle trajectories (i.e., rectilinear and streamline) indicates that deposit morphology varies significantly with particle trajectories, suggesting the possible necessity of including the particle inertial effect in the development of generalized correlations between pressure drop increase and the specific deposit.

It should be noted that the simulation was made with the assumption that particle trajectories were either rectilinear or follow streamlines. This obviously is an assumption and its use is open to question. On the other hand, it is recognized that the simulation in its present version does not provide sufficient accuracy to be quantitatively useful. For example, the effect of deposited particles on the flow field within the constricted tube was not considered. The inaccuracy in particle trajectory may lead to error in the prediction of the manner of the accumulation of deposited particles. It is hoped that on a macroscopic level, namely, when the change of the collection efficiency is related with the specific deposit, this error may not be significant. At the least, the results obtained with the use of the two limiting situations may provide a bound on the change of the collection efficiency. The experimental data shown in Fig. 13 seem to be in agreement with the argument.

COMPARISON WITH EXPERIMENTAL DATA

The validity and therefore the usefulness of the simulation can be assured only if it

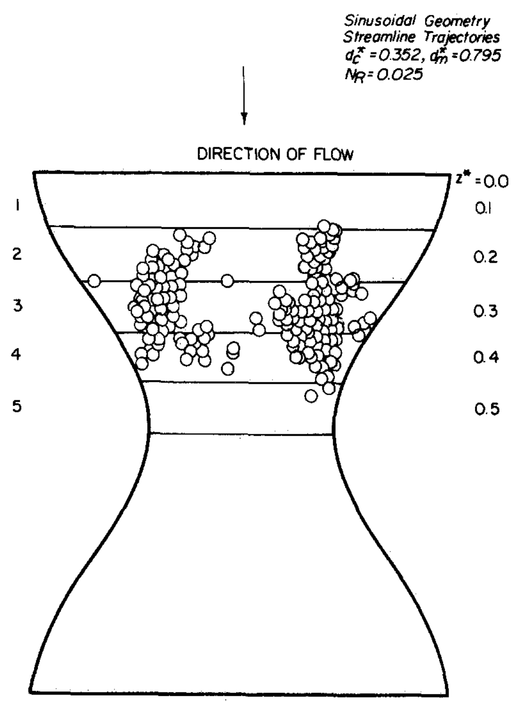

FIG. 12. Typical deposit pattern for streamline trajectories, side view.

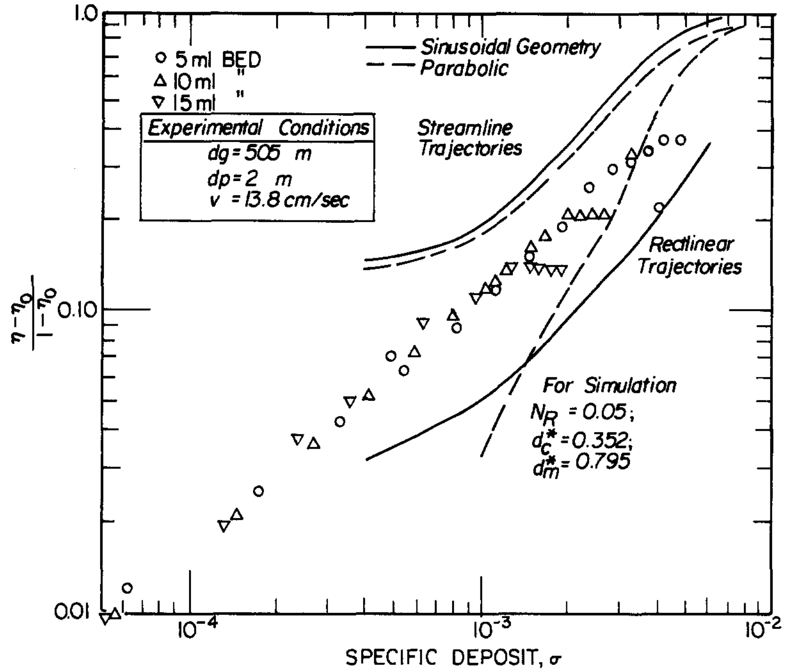

FIG. 13. Comparison between simulation model (Pendse, 1979) with experiments (Pannu, 1980).

agrees with experimental data. Since the simulation model yields a variety of information pertaining to both the macroscopic behavior of filter bed as well as detailed description of particle deposition, one could make different types of comparisons and to achieve different levels of model validation.

From a practical point of view, the relationship between the collection efficiency η and the extent of local deposition, σ is the most important piece of information necessary for the prediction of the performance of granular filters. A relationship between η vs σ can be readily obtained for a given set of physical and operating conditions with the precedure described before (i.e., Eqs. [17] and [20]). This information, in turn, can be compared with experimental data. Such a comparison is shown in Fig. 13. The data collected by Pannu (18) in his ongoing research were obtained by passing monodispersed aerosol suspensions (latex particles of size 1.03 μm) of low concentration (approximately 1000 particles/cm^3) through three experimental filters composed of nearly uniform glass spheres of diameter approximately 500 μm and a height of 0.44, 0.88, 1.32 cm, respectively. The particle concentrations of the influent and effluent streams were determined using a Climet particle counter (Model 208). The collection efficiency of the unit collector and the corresponding σ were obtained in the following manner. From the data obtained from the filter bed with the smallest height, σ were assumed to be uniformly distributed throughout the bed. The 0.88-cm bed was assumed to be a series of two beds, each with a height of 0.44 cm and the 1.32-cm height bed was considered to be a series of three 0.44 cm height beds. The consistency of unit collector efficiency obtained from experimental data with this assumption suggests that the uniform deposition assumption is justified.

The comparison between Pannu's data and the simulation model results has to be considered fairly good, even though the conditions under which the measurements were made and those used for simulation are not exactly the same. While it does not constitute a definite validation of the model, it does give credence to the model and justifies its further study.

POSSIBLE MODIFICATIONS AND FURTHER IMPROVEMENTS OF THE MODEL

The present model is formulated with the use of certain assumptions; the most important ones are: (1) The flow field within the unit collector does not change with the presence of deposited particles and (2) once an entering particle makes contact with the surface of the collector or an already deposited particle, the entering particle becomes automatically collected. It is obvious that justifications of these two assumptions need to be seriously considered.

The adhesion of a moving particle upon impact on a collecting surface has been examined by a number of investigators under different contexts. Loffler and Hiller (19) and Dahneke (20) among others have shown that for the case of aerosol particles impinging on a single fiber collector, particle adhesion is determined by the magnitude of the approaching velocity (normal component) for a given particle-fiber system. The recent work on fibrous model filters (21) has shown that the bouncing-off effect is indeed important and agreement between theory and experiment cannot be obtained without its inclusion. To what extent the bouncing-off effect is significant in granular filtration is not clear. The comparison as shown in Fig. 13 seems to indicate its relative unimportance. This perhaps can be justified that the interstitial velocity within a granular bed is much less than that in a fibrous bed. It should also be pointed out that the bouncing-off of an approaching particle does not necessarily mean that the particle will escape, since it may still be collected by other parts of the unit collector.

The presence of depositea particles within the unit collector obviously affects the flow field and this effect becomes more pronounced as the number of deposited particles increases. For the case of very high particle inertia, particle trajectories will remain rectilinear irrespective of the change in the flow field. The effect of omitting the deposited particles therefore is nil. On the other hand, if particle trajectories follow fluid streamlines, the use of a clean collector flow field will exaggerate the extent of particle collection. The results as shown in Fig. 13 are in agreement with this argument qualitatively.

The correct flow field within the unit collector with deposited particles, in principle, can be found from the solution of the relevant Navier–Stoker equations with appropriate boundary conditions. The mathematical complexities involved render such a direct approach impractical. Simplifications can be made if one assumes that the clean collection flow field expressions become invalid only when the amount of deposition becomes significant. Under such conditions, the outline of the deposit aggregates can be approximated by some simple geometry. Attempts have been made to consider particle deposition in clogged filter beds with the use of two spheres model (21, 22) and the results indicate that the omission of the effect of deposited particles may result in an overestimation of the collection efficiency by a factor of two. The validity of such analysis remains to be tested against appropriate experiments.

From a pragmatic point of view, more immediate and practical results perhaps can be obtained by extensively testing the simulation model against experimental data. Such comparisons would determine the conditions under which the approximations and simplifications used in this work are acceptable. If the trend observed in Fig. 13 is found to be generally true, it would be realistic to use the model for the study of the transient behavior of granular filtration. The problem of predicting the dynamic behavior of granular bed filters would be essentially solved. The collection of the necessary experimental data for such a test is being carried out at Syracuse at the present time.

APPENDIX 1: NOMENCLATURE

a_i	Coefficients of polynomial expression given by Eq. [18]
a_p	Particle radius
c	Particle concentrations (v/v)
d	Diameter of constricted tube
d_p	Particle diameter
d_g	Filter grain
d_c	Minimum diameter of constricted tube
d_i	Center-to-center distance between the ith deposited particle and the entering particles
d_m	Maximum diameter of constricted tube
d_c^*	Defined as d_c/d_g
d_m^*	Defined as d_m/d_g
$f(\bar{r}_i, \bar{r}_j)$	Factor accounting for the interaction between the ith and the jth deposited particles (see Eq. [29])
f_s	Friction factor for flow through pack bed—define $\left(-\frac{\partial p}{\partial z}\right)\frac{d_g}{2\rho V_s^2}$
$F_{D,0}$	Drag force on clean collector
G_1, G_2, G_3	Cumulative density functions for determining the initial position and size of entering particles
h	Height of unit collector
h^*	Defined as h/d_g
l	Unit bed element thickness
m_c	Number of particles collected per unit collector
m_{in}	Number of entering particles
N_c	Number of unit collectors per unit cross section of packed bed
N_c^*	Dimensionless N_c, definition given in Table I
N_R	Relative size parameter defined as d_p/d_g
N_{Re_s}	Reynolds number defined as $d_g V_s P/\mu$
p	Pressure
$\frac{\partial p}{\partial z}$	Pressure gradient
q	Volumetric flow into a unit collector
r	Radial coordinate
r_0	The maximum radial distance reached by a particle at the unit collector inlet
r_{in}	Radial coordinate of entering particles at inlet
$\bar{r}_i, \bar{r}_j, \bar{r}_k$	Position vectors of the ith, jth, and kth deposited particles, respectively
R_1, R_2, R_3	Random numbers uniformly distributed over (0, 1)
s	Standard deviation of particle size distribution
t	Time
V_c	Total volume of particles collected
$V_{(i)}$	Total volume of particles of a given size present in influent suspension
V_s	Superficial velocity of suspension flow through packed
y	Normal distance from particle to the surface of unit collector
z	z coordinate

Greek Letters

γ_0	Quantity defined by Eq. [25]
γ_i	Correction factor of the Stokes law drag force for deposited particles (Eq. [27])
ψ	Stream function
ψ^*	Dimensionless stream function
ψ_{in}	Value of stream function corresponding to the initial position of an entering particle
η	Collection efficiency of unit collector
η_0	Initial collection efficiency of unit collector
θ	Corrected time defined as

$t - \int_0^z \frac{\epsilon}{V_s} dz$ where ϵ is the bed porosity

μ Fluid viscosity

ρ Fluid density

σ Specific deposit, volume of deposited matter per unit bed volume

ACKNOWLEDGMENTS

The principle used in the formulation of the simulation model was developed as part of the study performed under Grants ENG-76-08755 and CPE 79-05962, National Science Foundation. The adaptation of the model to aerosol filtration in granular media was carried out under contract No. DE-A02-79-ER10386, Department of Energy, Office of Basic Energy Sciences.

REFERENCES

1. Juvinall, R. A., Kessie, R. W., and Steindler, M. J., "Sand Bed Filtration of Aerosols. A Review of Published Information on Their Use in Industrial and Atomic Facilities." ANL-7633, National Technical Information Service, Springfield, Virginia (1970).
2. Pendse, H., and Tien, C., "A Generalized Correlation for the Estimation of the Initial Collection Efficiency of Granular Filter Beds." Paper 56 AIChE Annual Meeting, Chicago (1980).
3. Thambimuthu, K. V., Doganoglu, Y., Farrokhalear, T., and Clift, R., "Aerosol Filtration in Fixed Granular Beds." Symposium of Deposition and Filtration of Particles from Gases and Liquids, Society of Chemical Industry, London, 107 (1978).
4. Gutfinger, C., Tardos, G. I., *Atmos. Environ.* **13,** 853 (1979).
5. Tardos, G. I., Yu, E., Pfeffer, R., and Squires, A. M., *J. Coll. Interface Sci.* **71,** 619 (1979).
6. Pendse, H., Tien, C., and Turian, R. M., *AIChE J.* **27,** 364 (1981).
7. Tien, C., Wang, C. S., and Barot, D. T., *Science* **196,** 183 (1977).
8. Wang, C. S., Beizaie, M., and Tien, C., *AIChE J.* **23,** 879 (1977).
9. Payatakes, A. C., Tien, C., and Turian, R. M., *AIChE* **19,** 58 (1973).
10. Fedkiw, P., and Newman, J., *AIChE J.* **23,** 255 (1977).
11. Venkatesan, M., and Rajagopalan, R., *AIChE J.* **26,** 694 (1980).
12. Payatakes, A. C., Tien, C., and Turian, R. M., *AIChE J.* **19,** 67 (1973).
13. Neira, M. A., and Payatakes, A. C., *AIChE J.* **24,** 43 (1978).
14. Chow, J. C. F., and Soda, K., *Phys. Fluids* **15,** 1700 (1972).
15. Tien, C., and Payatakes, A. C., *AIChE J.* **25,** 737 (1979).
16. Pendse, H., "A Study of Certain Problems Concerning Deep Bed Filtration." Ph.D. Dissertation, Syracuse University (1979).
17. Beizaie, M., "Particle Deposition on Single Collectors," Ph.D. Dissertation, Syracuse University (1977).
18. Pannu, J., Ph.D. Dissertation in Progress, Syracuse University (1980).
19. Loffler, F., "Problems and Recent Advances in Aerosol Filtration." Symposium on Separation Science and Technology for Energy Applications DOE and Oak Ridge National Laboratory, Gatlinberg, Tennessee (1979).
20. Dahneke, B., *J. Colloid Interface Sci.* **40,** 1 (1972).
21. Tsiang, R. C., "Mechanics of Particle Deposition on Model Filters Composed of an Array of Parallel Fibers." Ph.D. Dissertation, Syracuse University (1980).
22. Chiang, H. W., Ph.D. Dissertation in Progress, Syracuse University (1980).